



**Journal of  
Mechanics of  
Materials and Structures**

**NONUNIQUENESS AND INSTABILITY OF CLASSICAL FORMULATIONS OF  
NONASSOCIATED PLASTICITY, II: EFFECT OF NONTRADITIONAL  
PLASTICITY FEATURES ON THE SANDLER–RUBIN INSTABILITY**

Jeffrey Burghardt and Rebecca M. Brannon

**Volume 10, No. 2**

**March 2015**





## NONUNIQUENESS AND INSTABILITY OF CLASSICAL FORMULATIONS OF NONASSOCIATED PLASTICITY, II: EFFECT OF NONTRADITIONAL PLASTICITY FEATURES ON THE SANDLER–RUBIN INSTABILITY

JEFFREY BURGHARDT AND REBECCA M. BRANNON

In the companion article a case study problem was presented that illustrated a dynamic instability related to nonassociated plastic flow. This instability allows stress waves to grow in both amplitude and width as they propagate. In addition to this physically implausible behavior, multiple solutions to the equations of motion were shown to exist, which causes numerical solutions not to converge with mesh refinement. Reformulation of some aspects of traditional plasticity theory is necessary since associated models over-predict the amount of plastic dilatation, and nonassociated models may result in this physically unrealistic behavior. The case study solutions in the companion paper were limited to a few relatively simple plastic models. The purpose of this paper is to investigate the effects of various traditional and nontraditional plasticity features on the existence of the instability and resulting nonuniqueness. The instability and nonuniqueness are shown to persist with both hardening and softening. An incrementally nonlinear model is shown to eliminate the instability and result in mesh-independent solutions. A viscoplastic model is shown to lead to unstable solutions for all loading rates. However, mesh-independent numerical solutions are found when the loading timescale is much less than the plastic relaxation time. A nonlocal plasticity model is shown to produce solutions that are both unstable and mesh-dependent. Therefore, of the models considered, only the incrementally nonlinear model was capable of eliminating this nonphysical instability. This work provides much needed direction for laboratory investigations of the validity of incrementally nonlinear flow rules.

### 1. Introduction

An associated plasticity model is one for which the plastic strain rate tensor is proportional to the normal to the yield surface. While associated models have been shown to lead to unique solutions to boundary value problems [Hill 1958], several studies have demonstrated that associated flow rules are incompatible with experimental data.

Specifically, Spitzig et al. [1976] showed that associated models over-predict the amount of plastic dilatation in triaxial compression tests of metals. Lade et al. [1987] and Shen et al. [2012] found a similar problem with associated flow rules for geologic materials. More recently, it has been shown that nonassociated flow rules describe the anisotropic plastic flow of sheet metals better than associated flow rules [Stoughton 2002; Cvitanic et al. 2008; Mohr et al. 2010; Taherizadeh et al. 2010]. Additionally, Gao et al. [2011] have developed a plasticity model for aluminum 5083 and shown that, under a variety of loading conditions, a nonassociated model is in closer agreement with experimental data than is an associated model. However, several recent papers [Desmorat and Marull 2011; Dunand et al. 2012; Besse

---

*Keywords:* plasticity, flow rule, nonassociated flow rule, instability, incremental nonlinearity.

and Mohr 2012] have shown that a nonassociated flow rule is not necessary to describe the anisotropic plasticity of rolled sheet metal if other plasticity features are included. Popov and Lagoudas [2007] and Saint-Sulpice et al. [2009] found it necessary to use a nonassociated flow rule to describe the inelastic behavior of shape memory alloys, but more recently Saleeb et al. [2011] have developed and validated a shape memory alloy model utilizing an associated flow rule.

While these studies clearly represent a significant improvement upon more traditional metal plasticity models, Paquet et al. [2011] and Rousselier et al. [2012] describe several phenomena relating to the evolution of plastic anisotropy that are not well-described by even advanced macroscopic phenomenological plasticity models. Rousselier demonstrated that a model based on polycrystalline metal plasticity is capable of describing these complex behaviors. As noted in this recent work, when the material microstructure is accounted for, the yield surface can take on complex shapes, including the formation of vertices. At a vertex in the yield surface, the plastic flow direction depends upon the direction of loading and is therefore an irregular flow rule.

Many of these studies have demonstrated that certain nonassociated models are more compatible with experimental data than are similar associated models. This may be attributed to the additional mathematical flexibility of nonassociated models rather than to any physical arguments. This is well illustrated by the recent microscopically-based models discussed above.

Despite the fact that nonassociated models often fit experimental data better, the adoption of a nonassociated model brings with it a host of possible problems. For example, nonassociated models do not satisfy Drucker's stability postulate [1950] for all loading directions. Of course, Drucker's stability postulate is merely a sufficient, but not necessary, condition for stability and uniqueness. As discussed in detail below, nonassociated models have been shown to result in instability and a loss of uniqueness for certain loading conditions.

A well-known loading condition that results in both the loss of uniqueness of solution and instability with a nonassociated flow rule was discovered by Rudnicki and Rice [1975]. They showed that, under certain loading directions, a nonassociated model could result in a localization instability even while the material remained in the hardening regime. This localization instability has been shown to result in a loss of uniqueness of solution for local rate-independent plasticity models. This instability and nonuniqueness have been extensively studied over the years [Bažant 1976; de Borst et al. 1993; Dorgan 2006; Valanis 1998]. While the softening-like behavior of nonassociated models is consistent with experimental data, the governing equations are nevertheless ill-posed with the occurrence of this behavior and must be regularized in some way. The current leading regularization approaches appear to be nonlocal plasticity and gradient plasticity.

A related form of instability and loss of uniqueness of solution related to nonassociated plastic flow is the flutter instability [Bigoni 1995]. Whereas the localization instability occurs when a negative eigenvalue of the constitutive operator arises, the flutter instability occurs when a complex eigenvalue arises. For a more detailed discussion of the effect of nonassociated flow rules on the eigenvalues of the constitutive operator, see [Brannon and Drugan 1993]

Another, and fundamentally different, source of instability and nonuniqueness caused by nonassociated plastic flow was first observed by Sandler and Rubin [1987]. They showed that with any degree of nonassociativity there exist loading directions for which the wave speed in plastic loading exceeds the wave speed in elastic unloading. This over-stiffening occurs any time the trial stress rate tensor

has a positive inner product with the normal to the yield surface, but a negative inner product with the plastic strain rate tensor. This region of stress space, which lies above the yield surface, but below the plastic flow potential surface, will be herein referred to as the Sandler–Rubin wedge. Sandler and Rubin showed that the existence of these so-called “fast plastic” waves causes a loss of uniqueness of solutions and that solutions are admitted for which an infinitesimal stress perturbation can nonphysically grow in amplitude and width as it propagates. This phenomenon is essentially equivalent to spontaneous motion from a quiescent state, which can be construed as an implausible behavior for a passive material. Under these conditions all of the eigenvalues of the plastic tangent stiffness tensor are real and positive, so this phenomenon is not related to the localization or flutter instability previously discussed.

Nonetheless, the numerical manifestation of the ill-posedness caused by the Sandler–Rubin instability is remarkably similar to that caused by localization. Specifically, when a local model is used to solve a localization problem, the strain in the localization region becomes unbounded with mesh refinement. For localization problems, the region of unbounded strain is stationary in a Lagrangian sense. For the Sandler–Rubin instability, the region of unbounded strain lies at the peak of a propagating stress wave. As the head and tail of the wave diverge because of the inversion in plastic wave speeds, the region of unbounded strain expands linearly in time. In the one-dimensional problem considered in the companion paper, the solution in this region of space was shown to be subject to only two constraints:

$$0 \leq \dot{\sigma} \quad (1)$$

and

$$C_E < v < C_P, \quad (2)$$

where  $\dot{\sigma}$  is the axial component of the stress rate,  $C_E$  is the elastic wave speed,  $v$  is the wave speed in the region of nonuniqueness, and  $C_P$  is the plastic wave speed.

In a pair of relatively recent articles on plastic stability, Stoughton and Yoon [2006; 2008] have expressed some concerns about the range of validity of the Sandler–Rubin instability. In the second of these articles they suggest that the Sandler–Rubin instability is permitted by only a very small and simple subset of nonassociated plasticity models, and that any model with a nonconstant plastic wave speed will not be subject to the problems identified by Sandler and Rubin. In the companion paper it was shown via a numerical example that a model with nonlinear hardening, which produces a nonconstant plastic wave speed, results in the same problems that result with linear hardening.

In light of both the loss of uniqueness of solution and the physically implausible behavior permitted under the Sandler–Rubin instability, it seems that traditional nonassociated models must be rejected. However, as discussed previously, associated models also must be rejected since they are incompatible with experimental data. Clearly a resolution to this problem lies outside of traditional plasticity theories. The purpose of this paper is to investigate several nontraditional theories to determine which, if any, of these theories are capable of matching experimental data while at the same time eliminating the physically implausible Sandler–Rubin instability and resulting in unique solutions.

In part I of our paper, the existence and characteristics of the Sandler–Rubin instability were illustrated using both analytical and numerical solutions to a simple one-dimensional wave-propagation problem. To illustrate the instability in the simplest possible context, the companion paper employed a rate-independent, perfectly plastic, and nonlinear hardening model. In this paper we solve this same case study problem with a variety of generalizations of this simple model.

The case study problem of the companion paper is briefly described in Section 2. In Section 4, we examine various generalizations of the simple plasticity model considered in the companion article. The first of these generalizations discussed is a more detailed examination of hardening and softening than was presented in the companion paper. The second reformulation considered is the adoption of an incrementally nonlinear flow rule, which allows the plastic flow direction to change based on the incremental loading direction. The third alternative theory considered is the adoption of rate-dependence. The final reformulation of traditional plasticity theory considered here is an integral-type nonlocal plasticity theory.

## 2. Description of the case study problem from part I

In this section, a simple numerical case study problem is described that elicits the Sandler–Rubin instability. This case study problem, originally developed by Thomas Pučik, is described in greater detail in the companion article. The case study problem consists of a semi-infinite elastic/plastic half-space as shown in Figure 1. The axial component of the initial stress state  $\sigma_X^*$  is chosen to be  $-100$  MPa, while the lateral component,  $\sigma_Y^* = \sigma_Z^*$ , is chosen to be  $-17.55$  MPa, where stresses are taken to be positive in tension. The material is also assumed to be in a quiescent initial state. The linear Drucker–Prager yield function used in this case study is

$$f = \sqrt{J_2} + \alpha I_1 - k_o, \quad (3)$$

where  $J_2 = \frac{1}{2} \mathbf{S} : \mathbf{S}$ ,  $\mathbf{S}$  is the deviatoric stress tensor,  $I_1 = \text{Tr}(\boldsymbol{\sigma})$ , and  $\alpha$  and  $k_o$  are material parameters whose values are chosen to be 0.315 and 5.066 MPa respectively. With these parameters, and the chosen initial stress state, the material is at incipient yield in its initial condition. The dilatation angle is chosen to be zero, meaning that the plastic strain rate tensor is proportional to the deviatoric part of the stress tensor and therefore has no volumetric part. Various generalizations of this simple model will be considered and are discussed in detail below. This model was contrived to simplistically demonstrate the existence and character of the instability. In what follows, various enhancements to this model are systematically explored for the effect on the instability in this case study.

The surface traction at the free surface is initially  $-100$  MPa, which places the material in equilibrium in the initial state. A small perturbation is applied to the surface traction as shown in Figure 1. The perturbation is characterized by the peak change in stress  $\sigma_o = 10$  MPa, and the duration of the pulse  $\tau = 2$  ms. Since the axial component of stress changes from  $-100$  MPa to  $-90$  MPa, this is a tensile stress increment that reduces both the confining pressure and the magnitude of the stress deviator and induces plastic flow. This loading increment is reversed by returning the axial component of the stress tensor to its initial value in what can be shown to be an elastic recompression increment. This loading sequence results in the triangular-shaped time-history of the perturbation shown in Figure 1, with the front of the triangular pulse placing the material in a plastic loading state and the tail of the pulse placing the material in an elastic unloading state. Here loading refers to an increment that induces plastic flow and unloading refers to an increment that is purely elastic, even though the plastic loading increment represents a decrease in the applied load.

This perturbation causes a longitudinal wave to propagate through the half-space. As shown in the companion article, this loading condition places the trial stress rate in the Sandler–Rubin wedge and results in a plastic wave speed that exceeds the elastic wave speed. In the companion article this case study problem was shown to possess a two-parameter family of nonunique analytical solutions. The

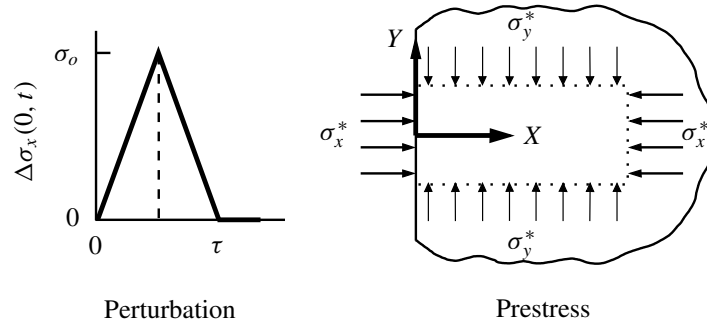


**Figure 1.** Geometry and loading for the case study problem.

problem was also solved numerically using the finite-element and material point methods. Figure 2 shows an example of the numerical solutions presented in the companion paper, which were found using the Uintah material point method (MPM) code [de St. Germain et al. 2000; Sulsky et al. 1994; Bardenhagen and Kober 2004], which is also used in the simulations presented in this paper.

As these solutions illustrate, the head of the wave (left-hand portion of the stress wave history) and the tail of the wave (right-hand portion of the stress wave history) are diverging from each other due to the plastic wave speed exceeding the elastic wave speed. This causes what is initially a single point at the top of the triangular stress pulse to open up into a finite region. It is in this region that the solution is nonunique. This nonuniqueness becomes apparent in analytical solutions by the presence of free parameters in the solution. In contrast, nonuniqueness can be much more subtle in numerical solutions. As with the nonuniqueness that occurs in localization problems, the numerical manifestation of the Sandler–Rubin instability occurs primarily through a mesh-dependency of the solution. This can be observed by comparing the coarse resolution plot on the left-hand side of Figure 2 with the finer resolution on the right-hand side of the same figure. At late times in the more resolved solution, secondary peaks in the stress wave begin to form, which grow much more rapidly than the primary peak. As the mesh is further

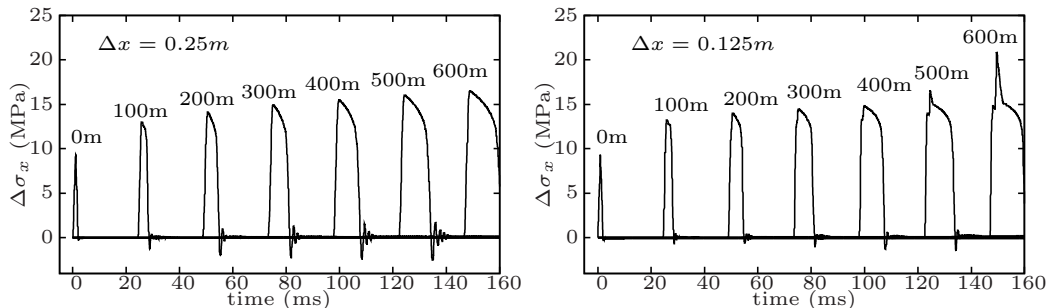


**Figure 2.** Stress histories at various locations throughout the problem domain using a local plasticity model, no hardening, and a mesh resolution of  $\Delta x = 0.25$  m (left) and  $\Delta x = 0.125$  m (right). This result was found using the Uintah MPM code and has been independently confirmed via analytical solutions and numerical solutions using a variety of FEM codes, as described in the companion paper.

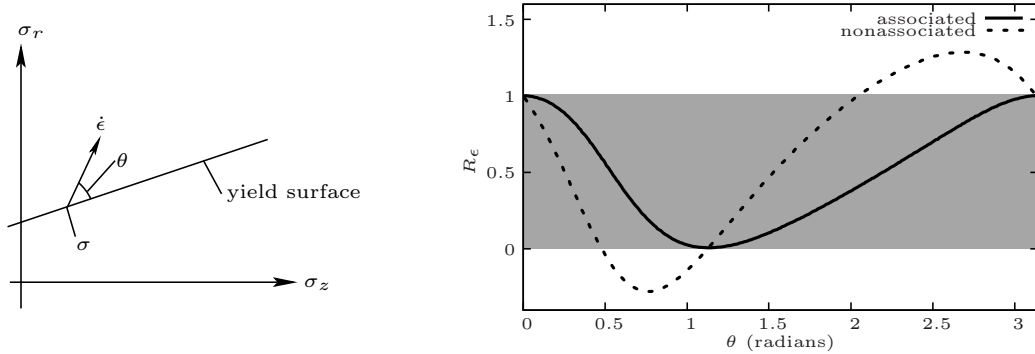


**Figure 3.** Directional stiffness ratio for nonhardening, associated and nonassociated linear Drucker–Prager models for all axisymmetric loading directions. Here  $\sigma_z = -(1/\sqrt{3}) \text{Tr}(\boldsymbol{\sigma})$  and  $\sigma_r = \|\boldsymbol{\sigma} - (1/3) \text{Tr}(\boldsymbol{\sigma})\|$ .

refined, these secondary peaks begin to form at earlier and earlier times and also grow at an increasingly rapid rate, with the result being that the numerical solution diverges with mesh refinement. The same trend was observed using several commercial finite-element codes, including DYNA3D and ABAQUS, though the formation of the secondary peaks began at a different mesh resolution with the FEM.

### 3. Directional stiffness

The concept of directional stiffness as developed by Runesson and Mroz [1989] is a convenient method for studying the stiffness properties of a plasticity model. The directional stiffness  $S_\epsilon$  is defined so that

$$\dot{\sigma}_\epsilon = S_\epsilon \dot{\epsilon}, \quad (4)$$

where  $\dot{\sigma}_\epsilon$  is the projection of the stress rate  $\dot{\sigma}$  onto the direction of  $\dot{\epsilon}$ . The directional stiffness ratio is defined as the ratio of the plastic and elastic directional stiffness:

$$R_\epsilon = \frac{S_\epsilon}{S_\epsilon^e} = \frac{\dot{\epsilon} : \mathbb{T} : \dot{\epsilon}}{\dot{\epsilon} : \mathbb{C} : \dot{\epsilon}}, \quad (5)$$

where  $S_\epsilon^e$  is the elastic directional stiffness,  $\mathbb{T}$  is the fourth-order elastic-plastic tangent stiffness tensor, and  $\mathbb{C}$  is the fourth-order elastic tangent stiffness tensor. This quantity provides a scalar measure of the stiffness of a plasticity model relative to the corresponding elastic stiffness for a given loading direction. As shown in Figure 3, the loading direction is quantified by the loading angle  $\theta$ , which is defined so that it is zero when the strain rate tensor is tangent to the yield surface. Of the two tangent directions,  $\theta$  is measured from the directional tangent tensor having a negative trace (compressive).

The right-hand side of Figure 3 is a plot of the directional stiffness ratio for both associated and nonassociated, perfectly plastic, linear Drucker–Prager models for  $0 \leq \theta \leq \pi$ .

As shown in the figure, the directional stiffness ratio for an associated model is always greater than zero and less than one. However, with a nonassociated model, the directional stiffness ratio is negative for some loading directions and greater than one for others. This results in the nonassociated model exhibiting a softening-like behavior for certain loading directions, and an over-stiffening behavior for



others. The softening-like behavior occurs when the plastic directional stiffness ratio is less than zero, and corresponds to the onset of localization even while the material remains in the hardening regime [Rudnicki and Rice 1975].

In contrast to the softening-like behavior, the over-stiffening behavior of nonassociated models has seen much less study, and its effects are much more subtle. As discussed in Section 2, when the over-stiffening behavior occurs, the plastic wave speed exceeds the elastic wave speed, resulting in a loss of uniqueness of solution and the existence of a physically implausible instability. The loss of uniqueness of solution itself is problematic from a practical standpoint as it can result in mesh-dependent numerical solutions, or solutions that are very sensitive to small changes in the input parameters, as is the case with localization problems. However, in contrast to the instability seen in localization problems, the Sandler–Rubin instability is not physically plausible. Therefore, resolving the mesh-dependency arising from the Sandler–Rubin instability is not a matter of only restoring the well-posedness, but rather the plasticity model must be modified to preclude the existence of the instability.

Therefore, we draw a conclusion that a realistic plasticity model will have a directional stiffness ratio that is less than zero for some loading directions (and therefore admits localization in the hardening regime), but is never greater than one (and therefore does not admit the Sandler–Rubin instability). We now examine various modifications to the elastic perfectly plastic model considered thus far to determine which, if either, of these requisite properties each model exhibits.

#### 4. Use of alternative theories

In what follows the case study problem is solved using the MPM with various modifications to the non-hardening plasticity model considered in the companion article. Both isotropic hardening and softening are considered, as well as three nontraditional plasticity model formulations. Each subsection describes the model reformulation as well and its effect upon the existence and characteristics of the Sandler–Rubin instability.

**4.1. *Hardening and softening.*** The companion paper considered only perfect plasticity and nonlinear hardening models. In this section we examine in more detail the effect of hardening, and additionally consider the effect of softening upon the Sandler–Rubin instability. Figure 4 shows the directional stiffness ratio for the modified constitutive model, including both hardening and softening. As has been pointed out by Runesson and Mroz [1989] and as witnessed by the increase in the minimum value of the directional stiffness ratio with hardening shown in Figure 4, hardening serves to diminish the softening-like behavior exhibited by nonassociated models. In fact, there exists a critical amount of hardening necessary to eliminate the possibility of attaining a negative value for the plastic directional stiffness, which in turn eliminates the possibility of localization. As would be expected, the figure shows that strain softening serves to increase the softening behavior of a nonassociated model (the minimum value of the directional stiffness ratio decreases with strain softening).

As shown in Figure 4, the maximum value of the directional stiffness ratio increases when the model includes softening. This means that the spurious stiffening caused by nonassociated models is exacerbated by softening. Therefore, softening would be expected to exacerbate the Sandler–Rubin instability. Hardening serves to slightly decrease the maximum value of the directional stiffness ratio. Therefore, hardening would be expected to ameliorate the Sandler–Rubin instability.

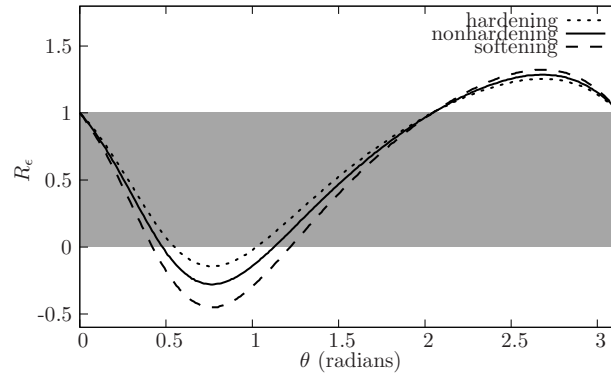


**Figure 4.** Directional stiffness ratio for a nonassociated model with softening, nonhardening (perfect plasticity) and hardening.

Figure 5 shows numerical solutions to the case study problem with hardening and softening. For reference, the perfect plasticity solution is also shown with dashed lines. As suggested by the increase in the maximum value of the directional stiffness ratio with softening shown in Figure 4, the plastic wave speed has increased as compared to the perfect plasticity solution. With this increase in plastic wave speed with softening, the degree of instability has also increased. In contrast, the solution with hardening shows a decrease in the plastic wave speed and a decrease in the degree of instability. It can be shown that only as the hardening modulus approaches infinity does the plastic wave speed approach the elastic wave speed. Therefore, in contrast to what was found with the localization instability, there is no critical amount of hardening or softening that eliminates the Sandler–Rubin instability. As mentioned above, in the companion paper it is shown that these same trends, along with the instability and nonuniqueness, persist with nonlinear hardening as well.

**4.2. Incrementally nonlinear plasticity.** While a large body of evidence suggests that the use of an associated flow rule is inappropriate for many materials [Spitzig et al. 1976; Lade et al. 1987], the physically implausible instability illustrated above is inherent in all nonassociated flow rules. Since both an associated and nonassociated flow rule seem to be at odds with experimental data, we ought to question the validity of the assumptions upon which both of these flow rules rest.

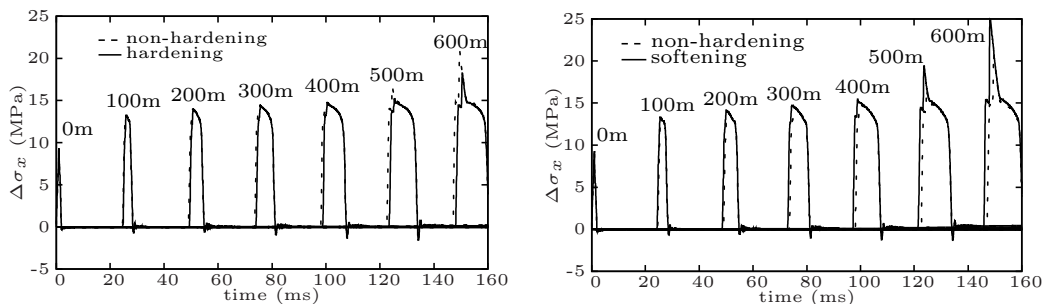


**Figure 5.** Stress histories for the numerical solution using hardening (left) and softening (right).

One such assumption is the existence of a *regular* flow rule. A regular flow rule is defined as one for which the direction of the plastic strain rate is independent of the direction of the strain rate itself. Of the very few studies to investigate the validity of this assumption, most have cast considerable doubt on the validity of a regular flow rule for general loading conditions [Anandarajah 1995; Tamagnini et al. 2005; Nicot and Darve 2007]. As noted above, the recent work by Rousselier et al. [2012] in polycrystalline metals plasticity, which can lead to an irregular flow rule, shows a significant improvement over macroscopic phenomenological models that use a regular flow rule. In addition to microscopic polycrystalline metals plasticity models, several macroscopic phenomenological incrementally nonlinear flow rules have been proposed in the literature [Hashiguchi 1997; Bauer 1996; Gudehus 1996; Ito 1979; Nicot and Darve 2007]. One of these, the “extended flow rule” (EFR) proposed by Hashiguchi [1997], is investigated as a possible alternative to the use of a regular rule. This flow rule was chosen since it may be easily incorporated within the basic framework of classical plasticity. The only difference is that the direction of the plastic strain rate is permitted to change based on the direction of the strain rate tensor. For this flow rule, the direction of the plastic strain rate  $\mathbf{M}$  is given by

$$\mathbf{M} = \hat{N} \|\dot{\mathbf{e}}^*\| + P_t^v \dot{e}_v \mathbf{I} + P_t^* \dot{\mathbf{e}}^*, \quad (6)$$

where  $\hat{N}$  is the unit normal to the yield surface,  $\|\cdot\|$  represents the Euclidean norm of its argument,  $\dot{\mathbf{e}}^*$  is the deviatoric part of the strain rate tensor,  $\dot{e}_v$  is the volumetric part of the strain rate tensor,  $\mathbf{I}$  is the identity tensor, and  $P_t^v$  and  $P_t^*$  are fitting parameters that control the degree to which the direction of plastic strain rate will be influenced by the direction of the strain rate tensor. Taking  $P_t^v$  and  $P_t^*$  to be zero would result in a regular, associated flow rule. By selecting nonzero values for one or both of these parameters the constitutive model may be calibrated so that it accurately predicts the volumetric strain observed in triaxial compression tests, while at the same time preventing the Sandler–Rubin instability by precluding the plastic wave speed from exceeding the elastic wave speed for any loading direction.

This flow rule was implemented using the Drucker–Prager constitutive model used in the example problem, with  $P_t^v = 0.5$  and  $P_t^* = 0$ . With these values, a triaxial compression test will result in very little volumetric plastic strain, as would be expected from a triaxial compression test on a rock-like material. The directional stiffness ratio for this model, and a perfectly plastic Drucker–Prager yield function, is shown on the left-hand side of Figure 6. For all loading directions, the directional stiffness ratio is less than one, indicating that no spurious stiffening is possible with this flow rule. The right-hand portion of this figure shows the stress histories for the case study problem with this flow rule. As expected by the boundedness of the directional stiffness ratio, no instability is evident with this flow rule. In fact the stress wave dissipates, rather than grows, as it propagates. Like a nonassociated flow rule, there are loading directions for which the directional stiffness ratio is negative. This means that this flow rule and choice of parameters will still admit localization for some loading directions. As mentioned above, the ability to localize while in the hardening regime is a desirable feature of a plasticity model.

While the EFR has the desirable attributes of disallowing the Sandler–Rubin instability, being capable of matching triaxial compression data and admitting the localization instability, such flow rules have undergone relatively little validation. Since an incrementally nonlinear flow rule is capable of *exactly* duplicating the triaxial compression response of a standard nonassociated model, triaxial compression tests alone will not validate or invalidate the EFR. The experimental measurements necessary to validate an incrementally nonlinear model are not straightforward. Additional data that measure the plastic strain

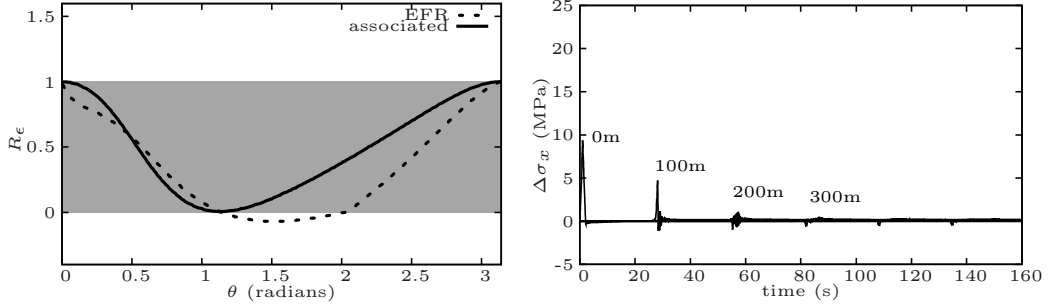


**Figure 6.** Left: stress histories every 100 meters through the problem domain using the extended flow rule (EFR) [Hashiguchi 1997] with  $P_v = 0.5$ . The wave rapidly dissipates since the plastic wave speed is less than the elastic. Right: The directional stiffness with the EFR for all axisymmetric directions. The stiffness is never greater than the elastic, but the stiffness is negative for some directions.

increments resulting from a variety of loading directions would be necessary to determine if the EFR is in fact valid. As discussed in our concluding remarks, such measurements may be critical to resolving the problems discussed in this paper, but performing such tests introduces irreducible uncertainty in the data. In the absence of such data, it would seem most prudent to choose a flow rule which disallows any nonphysical instabilities and can be fit to existing data.

**4.3. Rate-dependent plasticity.** In this section, we consider the effect of rate dependency on the existence and characteristics of the Sandler–Rubin instability. In their original work, Sandler and Rubin suggested that rate dependence might eliminate the nonphysical behavior caused by nonassociated plastic flow. The context of their suggestion was a discussion of the impacts of the Sandler–Rubin instability for quasistatic problems. The instability is inherently dynamic, but it is rational to demand that the quasistatic solution be admissible only if it is stable under infinitesimal dynamic perturbations. The conclusion is that, if a nonassociated flow rule is inappropriate for dynamic problems involving infinitesimal perturbations, then it also ought to be rejected for quasistatic problems. If rate dependence were shown to be capable of eliminating the instability for dynamic problems, then there would be no concern in using current rate-independent plasticity models for quasistatic problems.

With this motivation, the case study problem discussed above was solved using a rate-dependent generalized Duvaut–Lions overstress model. The generalized Duvaut–Lions model is an “overstress” model, meaning that, under high-rate loading, it allows the stress state to fall outside the yield surface. The “overstress” is quantified by

$$\boldsymbol{\sigma}^{\text{over}} = \boldsymbol{\sigma} - \boldsymbol{\sigma}^{\text{qs}}, \quad (7)$$

where  $\boldsymbol{\sigma}^{\text{qs}}$  is the corresponding quasistatic stress state. The strain rate  $\dot{\boldsymbol{\epsilon}}$  is additively decomposed into elastic ( $\dot{\boldsymbol{\epsilon}}^e$ ) and viscoplastic ( $\dot{\boldsymbol{\epsilon}}^{\text{vp}}$ ) components:

$$\dot{\boldsymbol{\epsilon}} = \dot{\boldsymbol{\epsilon}}^e + \dot{\boldsymbol{\epsilon}}^{\text{vp}}. \quad (8)$$

The elastic strain rate is defined to be the same as in rate-independent theory. The viscoplastic strain

rate is governed by

$$\dot{\epsilon}^{\text{vp}} = \frac{1}{\tau_{\text{mat}}} \mathbb{C}^{-1} : \boldsymbol{\sigma}^{\text{over}}, \quad (9)$$

where  $\tau_{\text{mat}}$  is the plastic relaxation time, and  $\mathbb{C}^{-1}$  is the inverse of the elastic tangent stiffness tensor (elastic tangent compliance tensor). The basis for this type of model is that plastic deformation requires a finite amount of time to develop. The time-scale associated with plastic deformation is quantified by  $\tau_{\text{mat}}$ . For a detailed description of this model see [Brannon 2007]. For rate-dependent models it is convenient to use the nondimensional Deborah number (De) to describe the loading rate. The Deborah number is defined as

$$\text{De} = \frac{\tau_{\text{mat}}}{\tau_{\text{load}}}, \quad (10)$$

where  $\tau_{\text{mat}}$  is the material relaxation time constant, and  $\tau_{\text{load}}$  is a time-scale associated with the loading. A large De indicates that the loading time-scale is short compared to the material relaxation time-scale, which would produce an elasticity-dominated response. A small De indicates that the loading time-scale is long compared to the material relaxation time-scale, which would produce a plasticity-dominated response. In the limit as  $\text{De} \rightarrow 0$ , a viscoplastic material model would predict a material response similar to a rate-independent model. In the limit as  $\text{De} \rightarrow \infty$ , a viscoplastic material model would predict a response that is purely elastic. Whereas, at high De, the rate-dependency will cause a viscoplastic material model to predict a more elastic-like response.

Figure 7 shows a series of plots of the stress history at various locations in the problem domain using several values of De. As discussed above, for low De, the material behavior would be expected to be similar to the rate-independent response. However, for this case study problem the solution is nonunique across the peak of the wave. This fact allows the solution in this region to change dramatically with even small changes in the material response. This is evident in the stress histories for  $\text{De} = 0.01$  shown in Figure 7. As would be expected, the head and tail of the wave are propagating with essentially the same speed as with the rate-independent solution (dashed line). However, the numerical solution across the peak of the wave is dramatically different than with the rate-independent model, and has become much more unstable. Again, this should not be cause for concern since no unique solution exists for this region of  $(x, t)$  space. As discussed in Section 2, the only constraints on the solution in this region are that the stress rate be greater than or equal to zero, and that the wave speed be greater than the elastic wave speed and less than the plastic wave speed. The numerical solution for  $\text{De} = 0.01$  shown in Figure 7 satisfies both of these constraints.

When the relaxation time is nearly the same as the loading rate, the material behavior would be expected to become more elastic. This can be seen in the stress history plots for  $\text{De} = 1$  shown in Figure 7. For this solution the head and tail of the wave are diverging at a much lower rate, and are propagating with a wave speed that lies between the elastic and plastic wave speeds. Because the actual stress state can transiently lie outside the yield surface with the viscoplasticity formulation used, the viscoplastic strain rate can be nonzero even when the quasistatic stress state is within the yield surface. After the quasistatic stress state enters the yield surface, the overstress will exponentially decay to zero so that the actual stress state will approach the quasistatic stress state as it moves to an elastic state. The rate at which this approach occurs depends upon the relaxation time. Therefore, when the relaxation time is of the same order as the loading rate, a large part of the tail of the wave may still be undergoing

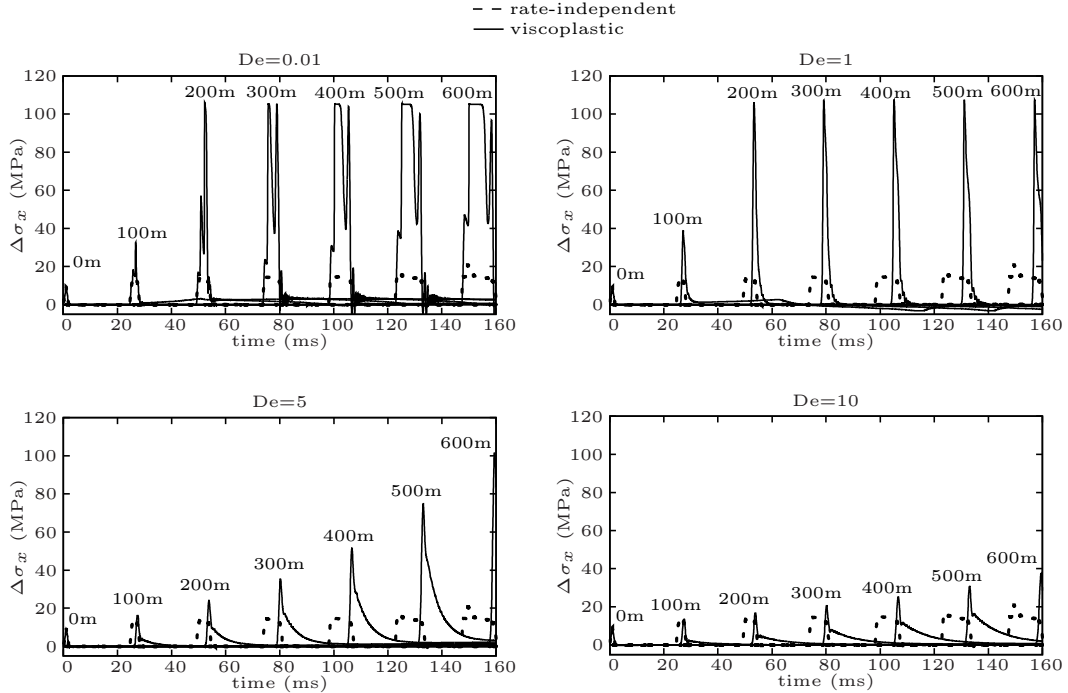


**Figure 7.** Stress histories for a Duvaut–Lions viscoplasticity model for  $De = 0.01$  (top left),  $De = 1$  (top right),  $De = 5$  (bottom left), and  $De = 10$  (bottom right).

viscoplastic deformation, even though the quasistatic stress state is within the yield surface. This is why the tail of the wave becomes increasingly dispersed as  $De$  increases, as seen in Figure 7. This also causes an increasing portion of the tail of the wave to be in a viscoplastic state as  $De$  increases. This also reduces the rate at which the head and tail of the wave diverge at high  $De$ , thereby decreasing the degree of instability in the solution. Also, for the mesh resolutions considered ( $\Delta x = 2$  m to  $\Delta x = 0.125$  m), the numerical solutions for  $De > 5$  seemed to converge to a unique solution, although the instability remains.

**4.4. Nonlocal plasticity.** As was mentioned in Section 1, there are two known instabilities that may arise from nonassociated plasticity models: a localization instability and the Sandler–Rubin instability. As was mentioned previously, despite the fact that these two instabilities arise from essentially opposite effects (softening-like behavior versus excessive stiffening behavior), their numerical manifestations have some similarities. With both the localization and the Sandler–Rubin instability the strain becomes unbounded inside a discrete region of space. In both cases the governing equations become ill-posed.

In the case of the localization, the instability is an actual phenomenon that a realistic model ought to admit. Nonetheless, to achieve unique solutions to localization problems, some modification of the model is required to regularize the governing equations. Two commonly used approaches to regularizing localization problems are nonlocal plasticity and gradient plasticity. Both of these modifications to traditional plasticity theory cause wave propagation to become dispersive, which means that waves of different frequencies propagate at different velocities. Dispersive wave propagation behavior has been

shown to be critical to allowing these types of models to lead to mesh-independent numerical solutions to localization problems [Sluys et al. 1993; Di Luzio and Bažant 2005].

In this section, we investigate the effect of nonlocal plasticity and the resulting dispersive wave propagation behavior on the Sandler–Rubin instability. This is done by solving our case study problem using an integral-type overlocal plasticity model as described by Strömberg and Ristinmaa [1996]. An overlocal model includes both local hardening/softening and nonlocal hardening/softening. The overlocal Drucker–Prager yield function is given by

$$f = \sqrt{J_2} + \alpha I_1 - k_o - (1 - m)\eta + m\zeta, \quad (11)$$

where  $\eta$  is the local hardening/softening function,  $\zeta$  is the nonlocal hardening/softening function, and  $m$  is the overlocal parameter. For  $m = 0$ , a purely local model is obtained, and for  $m = 1$  a purely nonlocal model is obtained. As discussed by both Strömberg and Ristinmaa [1996] and Di Luzio and Bažant [2005], the best localization limiting properties are obtained with the overlocal choice,  $m > 1$ . In this paper we use  $m = 2$ . The hardening/softening functions evolve according to

$$\dot{\eta}(\mathbf{x}) = h\dot{\lambda}(\mathbf{x}) \quad (12)$$

and

$$\dot{\zeta}(\mathbf{x}) = \frac{h}{V_\alpha} \int_{\Omega} \alpha(\mathbf{x} - \mathbf{s}) \dot{\lambda}(\mathbf{s}) dV, \quad (13)$$

where  $\mathbf{x}$  is the position vector of a given material particle,  $h$  is the hardening/softening modulus (here taken to be a constant material parameter),  $V_\alpha = \int_{\Omega} \alpha(\mathbf{s}) dV$ , and  $\alpha(\mathbf{x})$  is the nonlocal weighting function, here chosen to be the Gaussian distribution function given by

$$\alpha(\mathbf{x}) = \text{Exp}[-k\|\mathbf{x}\|/l]^2, \quad (14)$$

where  $k = (6\sqrt{\pi})^{1/3}$ , and  $l$  is the nonlocal length scale. With the nonlocal term, the yield function at each material point becomes coupled with all material points within the support of  $\alpha(\mathbf{x})$ . To solve this coupled set of equations, a new fixed-point iteration scheme (to be documented in a separate article) was developed and implemented into the MPM solution procedure.

A perturbation analysis technique described by Di Luzio and Bažant [2005], was adapted to solve for the frequency-dependent wave propagation velocity for the uniaxial strain wave propagation problem in this paper. The left-hand side of Figure 8 shows the resulting wave propagation velocity versus frequency for the nonlocal Drucker–Prager model. Unlike the dispersion relations for localization problems reported in the literature which focused on low values of the directional stiffness ratio, with the overlocal Drucker–Prager model at high directional stiffness ratios no localization occurs. Hence there is no critical wave frequency at which the propagation speed is zero. This is due to the over-stiffening behavior of the nonassociated model for the loading directions involved in this problem. The wave propagation velocity is bounded by the purely local softening wave speed (upper bound) and by the purely local wave speed (lower bound). This is because with low frequencies (and therefore small gradients) the nonlocal average of the plastic strain approaches the local value, so the nonlocal model results in little change as compared to a purely local softening model. For high frequency waves the nonlocal average for a material particle will be much less than the local value since neighboring “elastic” particles, whose plastic strain rate

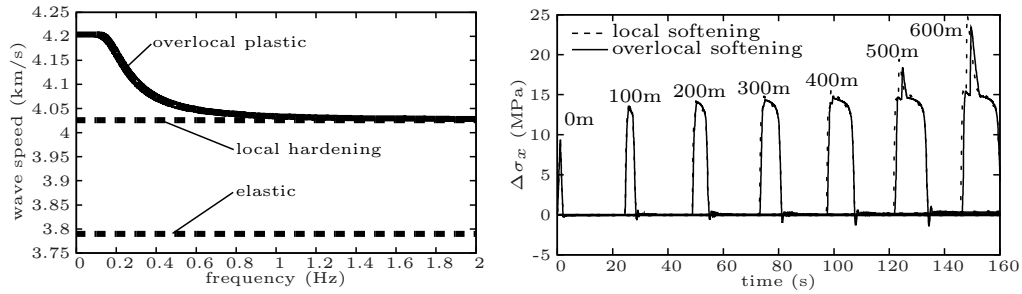


**Figure 8.** A plot of the frequency-dependent wave propagation velocity for the case study problem with an overlocal plasticity model, with the elastic and local hardening wave speeds shown for reference (left). Stress histories using an overlocal plasticity model with a nonlocal length scale of 1 m and a mesh resolution of 0.125 m (right).

tensor is zero, are included in the average. Therefore, for high frequencies, the local term of the overlocal hardening/softening dominates, and the response approaches that of a local hardening model.

The case study was solved using a nonlocal length scale of  $l = 1.0$  m. The internal length scale is proportional to the length scale associated with a critical material microstructure. The critical material length scale depends upon the length scale associated with the problem geometry and the wave length of the solution. This case study problem is meant to represent a stress wave propagating through geologic strata. For the length scales involved and the frequency of the solution, the critical material structure driving the nonlocal length scale would likely be the thickness of bedding planes or similar geologic structures. With this in mind a nonlocal length scale of one meter would be reasonable.

The right-hand side of Figure 8 shows the stress histories at various locations in the problem domain using the overlocal model discussed above. For reference, the local softening solution is shown with a dashed line. Consistent with the dispersion plot in the same figure, the overlocal model has resulted in a reduction in the plastic wave speed relative to the local softening solution; nevertheless, the instability and nonuniqueness persist. As can be seen by the horizontal separation of the curves in Figure 8, the difference in arrival time is greater for the secondary pulse that it is for the primary pulse. This is due to the higher frequency of the secondary pulse, which, according to the dispersion relation for this problem, results in a decrease in wave speed as compared to lower frequency waves.

From the dispersion relation and the overlocal case study solution, we conclude that a nonlocal plasticity model eliminates neither the Sandler–Rubin instability nor the resulting ill-posedness.

## 5. Concluding remarks

Of the models considered, only Hashiguchi’s incrementally nonlinear extended flow rule (EFR) [Hashiguchi 1997] eliminated the Sandler–Rubin instability. The viscoplastic model considered here resulted in mesh-independent solutions for high loading rates, but the nonphysical instability was present for all loading rates considered. Both the instability and the mesh dependency of the numerical solution were observed with both hardening and softening. Hardening was shown to diminish, but not eliminate, the instability, while softening tended to exacerbate it. The nonlocal plasticity solutions were very similar to the local plasticity solutions. Therefore, of the models considered here, the incrementally nonlinear



flow rule is the only one that may eliminate the instability while maintaining the desirable aspects of a nonassociated model.

As discussed in Section 4.2, Hashiguchi's EFR model introduces new material parameters that must be calibrated to a material of interest. To choose these parameters for a given material, the plastic strain increment must be measured for several loading directions. To measure the plastic strain increments, laboratory tests much include unloading increments. Furthermore, to measure these increments at the same material state for a different loading direction requires nonproportional loading. A limited amount of such data is available in the literature, and collecting such data is complicated by the loading-history dependent nature of plastic loading [Brannon et al. 2009].

Measuring the components of any tensor (in our case the tangent stiffness) requires measuring the response to more than one loading direction. In measuring the plastic strain increment for one loading direction, however, the material is permanently altered, making it impossible to know how the material would have responded to a different loading direction from the same initial state. Any further loading of the material with a loading increment in a different direction begins at a different material state, therefore it is impossible to measure the tangent stiffness in the laboratory with certainty. Stoughton [2002, p. 689] pointed out a few additional problems with making such measurements. Specifically, he mentioned that many materials of interest do not exhibit a "sharp" yield point, but instead the material gradually transitions from elastic to elastic/plastic deformation. This makes detecting the onset of yield difficult. Several techniques have been used to ameliorate the these problem, each with its own drawbacks [Anandarajah 1995; Tamagnini et al. 2005; Brannon et al. 2009].

The flow rule validation studies from the sheet metal forming community [Mohr et al. 2010; Dunand and Mohr 2011; Taherizadeh et al. 2010] have performed a best-fit parametrization of associated and nonassociated regular flow rule models to a subset of their experimental data. The models were then used to generate predictions for other experimental data that were not used for model calibration. As mentioned previously, these studies have shown that a nonassociated flow rule is better able to match the experimental data. Although these tests were performed for a wide variety of loading directions, none of these tests explicitly measured the plastic strain increments by including unloading increments. These and other tests already mentioned do provide a compelling case against an associated flow rule, but they do not provide any evidence for or against the validity of a regular flow rule.

To our knowledge, no study has conclusively validated or invalidated the existence of a regular flow rule. Therefore, the validity of the incrementally nonlinear approach is a critical topic for future experimental work. It is suggested that future validation efforts include incrementally nonlinear models as a possible alternative to traditional regular flow rules. Until such experimental evidence becomes available, it seems prudent to choose a model that fits known data while at the same time disallowing the nonphysical instabilities evident in traditional nonassociated plasticity. Therefore, analysts may consider adopting an incrementally nonlinear approach if an analysis involves loading paths in the directions which could potentially excite the Sandler–Rubin instability.

## 6. Acknowledgments

The authors wish to acknowledge the keen insights and encouragement of Dr. Thomas A. Pučík for inspiring this work, and to thank Noreen Pučík for her assistance and encouragement to publish her late

husband's final work. The authors also wish to acknowledge the financial support of Sandia National Laboratories.

### References

- [Anandarajah 1995] A. Anandarajah, "Incremental stress-strain behavior of granular soil", *J. Geotech. Eng. (ASCE)* **121**:1 (1995), 57–68.
- [Bardenhagen and Kober 2004] S. G. Bardenhagen and E. M. Kober, "The generalized interpolation material point method", *Comput. Model. Eng. Sci.* **5**:6 (2004), 477–495.
- [Bauer 1996] E. Bauer, "Calibration of a comprehensive hypoplastic model for granular materials", *Soils Found.* **36**:1 (1996), 13–26.
- [Bažant 1976] Z. P. Bažant, "Instability, ductility, and size effect in strain-softening concrete", *J. Eng. Mech. Div. (ASCE)* **102**:2 (1976), 331–344.
- [Besse and Mohr 2012] C. C. Besse and D. Mohr, "Plasticity of formable all-metal sandwich sheets: Virtual experiments and constitutive modeling", *Int. J. Solids Struct.* **49**:19–20 (2012), 2863–2880.
- [Bigoni 1995] D. Bigoni, "On flutter instability in elastoplastic constitutive models", *Int. J. Solids Struct.* **32**:21 (1995), 3167–3189.
- [de Borst et al. 1993] R. de Borst, L. J. Sluys, H. B. Muhlhaus, and J. Pamin, "Fundamental issues in finite element analyses of localization of deformation", *Eng. Computation.* **10**:2 (1993), 99–121.
- [Brannon 2007] R. M. Brannon, "Elements of phenomenological plasticity: Geometrical insight, computational algorithms, and topics in shock physics", pp. 225–274 in *Shockwave science and technology reference library*, edited by Y. Horie, Springer, Berlin, 2007.
- [Brannon and Drugan 1993] R. M. Brannon and W. J. Drugan, "Influence of nonclassical elastic-plastic constitutive features on shock wave existence and spectral solutions", *J. Mech. Phys. Solids* **41**:2 (1993), 297–330.
- [Brannon et al. 2009] R. Brannon, J. Burghardt, D. Bronowski, and S. Bauer, "Experimental assessment of unvalidated assumptions in classical plasticity theory", Report SAND2009-0351, Sandia National Laboratory, 2009, Available at <http://tinyurl.com/brannon2009>.
- [Cvitanic et al. 2008] V. Cvitanic, F. Vlak, and Z. Lozina, "A finite element formulation based on non-associated plasticity for sheet metal forming", *Int. J. Plast.* **24**:4 (2008), 646–687.
- [Desmorat and Marull 2011] R. Desmorat and R. Marull, "Non-quadratic Kelvin modes based plasticity criteria for anisotropic materials", *Int. J. Plast.* **27**:3 (2011), 328–351.
- [Di Luzio and Bažant 2005] G. Di Luzio and Z. P. Bažant, "Spectral analysis of localization in nonlocal and over-nonlocal materials with softening plasticity or damage", *Int. J. Solids Struct.* **42**:23 (2005), 6071–6100.
- [Dorgan 2006] R. J. Dorgan, "A mixed finite element implementation of a gradient-enhanced coupled damage–plasticity model", *Int. J. Damage Mech.* **15**:3 (2006), 201–235.
- [Drucker 1950] D. C. Drucker, "Some implications of work hardening and ideal plasticity", *Quart. Appl. Math.* **7** (1950), 411–418.
- [Dunand and Mohr 2011] M. Dunand and D. Mohr, "On the predictive capabilities of the shear modified Gurson and the modified Mohr–Coulomb fracture models over a wide range of stress triaxialities and Lode angles", *J. Mech. Phys. Solids* **59**:7 (2011), 1374–1394.
- [Dunand et al. 2012] M. Dunand, A. P. Maertens, M. Luo, and D. Mohr, "Experiments and modeling of anisotropic aluminum extrusions under multiaxial loading Part I: Plasticity", *Int. J. Plast.* **36** (2012), 34–49.
- [Gao et al. 2011] X. Gao, T. Zhang, J. Zhou, S. M. Graham, M. Hayden, and C. Roe, "On stress-state dependent plasticity modeling: Significance of the hydrostatic stress, the third invariant of stress deviator and the non-associated flow rule", *Int. J. Plast.* **27**:2 (2011), 217–231.
- [Gudehus 1996] G. Gudehus, "Comprehensive constitutive equation for granular materials", *Soils Found.* **36**:1 (1996), 1–12.
- [Hashiguchi 1997] K. Hashiguchi, "The extended flow rule in plasticity", *Int. J. Plast.* **13**:1–2 (1997), 37–58.

- [Hill 1958] R. Hill, "A general theory of uniqueness and stability in elastic-plastic solids", *J. Mech. Phys. Solids* **6**:3 (1958), 236–249.
- [Ito 1979] K. Ito, "New flow rule for an elastic-plastic solid based on KBW model with a view to lowering the buckling stresses of plates or shells", *Tech. Rep. Tohoku Univ.* **44**:2 (1979), 199–232.
- [Lade et al. 1987] P. V. Lade, R. B. Nelson, and Y. M. Ito, "Nonassociated flow and stability of granular materials", *J. Eng. Mech. (ASCE)* **113**:9 (1987), 1302–1318.
- [Mohr et al. 2010] D. Mohr, M. Dunand, and K.-H. Kim, "Evaluation of associated and non-associated quadratic plasticity models for advanced high strength steel sheets under multi-axial loading", *Int. J. Plast.* **26**:7 (2010), 939–956.
- [Nicot and Darve 2007] F. Nicot and F. Darve, "Basic features of plastic strains: From micro-mechanics to incrementally nonlinear models", *Int. J. Plast.* **23**:9 (2007), 1555–1588.
- [Paquet et al. 2011] D. Paquet, P. Dondeti, and S. Ghosh, "Dual-stage nested homogenization for rate-dependent anisotropic elasto-plasticity model of dendritic cast aluminum alloys", *Int. J. Plast.* **27**:10 (2011), 1677–1701.
- [Popov and Lagoudas 2007] P. Popov and D. C. Lagoudas, "A 3-D constitutive model for shape memory alloys incorporating pseudoelasticity and detwinning of self-accommodated martensite", *Int. J. Plast.* **23**:10–11 (2007), 1679–1720.
- [Rousselier et al. 2012] G. Rousselier, M. Luo, and D. Mohr, "Macroscopic plasticity modeling of anisotropic aluminum extrusions using a reduced texture methodology", *Int. J. Plast.* **30–31** (2012), 144–165.
- [Rudnicki and Rice 1975] J. Rudnicki and J. R. Rice, "Conditions for the localization of deformation in pressure-sensitive dilatant materials", *J. Mech. Phys. Solids* **23**:6 (1975), 371–394.
- [Runesson and Mroz 1989] K. Runesson and Z. Mroz, "A note on nonassociated plastic flow rules", *Int. J. Plast.* **5**:6 (1989), 639–658.
- [Saint-Sulpice et al. 2009] L. Saint-Sulpice, S. A. Chirani, and S. Calloch, "A 3D super-elastic model for shape memory alloys taking into account progressive strain under cyclic loadings", *Mech. Mater.* **41**:1 (2009), 12–26.
- [Saleeb et al. 2011] A. F. Saleeb, S. A. P. II, and A. Kumar, "A multi-axial, multimechanism based constitutive model for the comprehensive representation of the evolutionary response of SMAs under general thermomechanical loading conditions", *Int. J. Plast.* **27**:5 (2011), 655–687.
- [Sandler and Rubin 1987] I. S. Sandler and D. Rubin, "The consequences of non-associated plasticity in dynamic problems", pp. 345–353 in *Constitutive laws for engineering materials* (Tucson, AZ), edited by C. Desai, Elsevier, Amsterdam, 1987.
- [Shen et al. 2012] W. Q. Shen, J. F. Shao, D. Kondo, and B. Gatmiri, "A micro-macro model for clayey rocks with a plastic compressible porous matrix", *Int. J. Plast.* **36** (2012), 64–85.
- [Sluys et al. 1993] L. J. Sluys, R. de Borst, and H. B. Huhlhaus, "Wave propagation, localization and dispersion in a gradient-dependent medium", *Int. J. Solids Struct.* **30**:9 (1993), 1153–1171.
- [Spitzig et al. 1976] W. A. Spitzig, R. J. Sober, and O. Richmond, "The effect of hydrostatic pressure on the deformation behavior of maraging and HY-80 steels and its implications for plasticity theory", *Metall. Trans. A* **7**:11 (1976), 1703–1710.
- [de St. Germain et al. 2000] J. D. de St. Germain, J. McCorquodale, S. G. Parker, and C. R. Johnson, "Uintah: A massively parallel problem solving environment", pp. 33–41 in *Ninth IEEE international symposium on high performance and distributed computing* (Pittsburgh, PA, 2000), edited by B. Werner, IEEE, Piscataway, NJ, 2000.
- [Stoughton 2002] T. B. Stoughton, "A non-associated flow rule for sheet metal forming", *Int. J. Plast.* **18**:5–6 (2002), 687–714.
- [Stoughton and Yoon 2006] T. B. Stoughton and J. W. Yoon, "Review of Drucker's postulate and the issue of plastic stability in metal forming", *Int. J. Plast.* **22**:3 (2006), 391–433.
- [Stoughton and Yoon 2008] T. B. Stoughton and J. W. Yoon, "On the existence of indeterminate solutions to the equations of motion under non-associated flow", *Int. J. Plast.* **24**:4 (2008), 583–613.
- [Strömberg and Ristinmaa 1996] L. Strömberg and M. Ristinmaa, "FE-formulation of a nonlocal plasticity theory", *Comput. Methods Appl. Mech. Eng.* **136**:1-2 (1996), 127–144.
- [Sulsky et al. 1994] D. Sulsky, Z. Chen, and H. L. Schreyer, "A particle method for history-dependent materials", *Comput. Methods Appl. Mech. Eng.* **118**:1-2 (1994), 179–196.
- [Taherizadeh et al. 2010] A. Taherizadeh, D. E. Green, A. Ghaei, and J.-W. Yoon, "A non-associated constitutive model with mixed iso-kinematic hardening for finite element simulation of sheet metal forming", *Int. J. Plast.* **26**:2 (2010), 288–309.

[Tamagnini et al. 2005] C. Tamagnini, F. Calvetti, and G. Viggiani, “An assessment of plasticity theories for modeling the incrementally nonlinear behavior of granular soils”, *J. Eng. Math.* **52**:1-3 (2005), 265–291.

[Valanis 1998] K. C. Valanis, “Diffusion potential and well-posedness in non-associative plasticity”, *Int. J. Solids Struct.* **35**:36 (1998), 5173–5188.

Received 2 Jul 2014. Revised 15 Mar 2015. Accepted 4 Apr 2015.

JEFFREY BURGHARDT: [jburghardt@slb.com](mailto:jburghardt@slb.com)

*Schlumberger, 1935 S. Fremont Dr., Salt Lake City, UT 84104, United States*

REBECCA M. BRANNON: [rebecca.brannon@utah.edu](mailto:rebecca.brannon@utah.edu)

*University of Utah, 50 S. Campus Dr., Salt Lake City, UT 84108, United States*

# JOURNAL OF MECHANICS OF MATERIALS AND STRUCTURES

[msp.org/jomms](http://msp.org/jomms)

Founded by Charles R. Steele and Marie-Louise Steele

## EDITORIAL BOARD

ADAIR R. AGUIAR	University of São Paulo at São Carlos, Brazil
KATIA BERTOLDI	Harvard University, USA
DAVIDE BIGONI	University of Trento, Italy
YIBIN FU	Keele University, UK
IWONA JASIUK	University of Illinois at Urbana-Champaign, USA
C. W. LIM	City University of Hong Kong
THOMAS J. PENCE	Michigan State University, USA
DAVID STEIGMANN	University of California at Berkeley, USA

## ADVISORY BOARD

J. P. CARTER	University of Sydney, Australia
D. H. HODGES	Georgia Institute of Technology, USA
J. HUTCHINSON	Harvard University, USA
D. PAMPLONA	Universidade Católica do Rio de Janeiro, Brazil
M. B. RUBIN	Technion, Haifa, Israel

**PRODUCTION** [production@msp.org](mailto:production@msp.org)

SILVIO LEVY Scientific Editor

Cover photo: Ev Shafir

---

See [msp.org/jomms](http://msp.org/jomms) for submission guidelines.

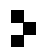
---

JoMMS (ISSN 1559-3959) at Mathematical Sciences Publishers, 798 Evans Hall #6840, c/o University of California, Berkeley, CA 94720-3840, is published in 10 issues a year. The subscription price for 2015 is US\$565/year for the electronic version, and \$725/year (+\$60, if shipping outside the US) for print and electronic. Subscriptions, requests for back issues, and changes of address should be sent to MSP.

---

JoMMS peer-review and production is managed by EditFLOW® from Mathematical Sciences Publishers.

PUBLISHED BY

 **mathematical sciences publishers**  
nonprofit scientific publishing

<http://msp.org/>

© 2015 Mathematical Sciences Publishers

# Journal of Mechanics of Materials and Structures

Volume 10, No. 2

March 2015

---

- On the vibration simulation of submerged pipes: Structural health monitoring aspects** PEJMAN RAZI and FARID TAHERI 105
- Nonuniqueness and instability of classical formulations of nonassociated plasticity I: Case study** THOMAS PUČIK, REBECCA M. BRANNON and JEFFREY BURGARDT 123
- Nonuniqueness and instability of classical formulations of nonassociated plasticity II: Effect of nontraditional plasticity features on the Sandler–Rubin instability** JEFFREY BURGARDT and REBECCA M. BRANNON 149
- Peridynamics for antiplane shear and torsional deformations** SELDA OTERKUS and ERDOGAN MADENCI 167
- A hysteretic Bingham model for MR dampers to control cable vibrations** SELSEBIL SOLTANE, SAMI MONTASSAR, OTHMAN BEN MEKKI and RACHED EL FATMI 195



1559-3959(2015)10:2;1-B